Spin-Coupled Study of the Electronic Mechanism of the Hetero-Diels−Alder Reaction of Acrolein and Ethene

Joshua J. Blavins,[†] David L. Cooper,*[,‡] and Peter B. Karadakov*[,†]

Department of Chemistry, University of York, Heslington, York, YO10 5DD, U.K., and Department of Chemistry, University of Liverpool, Liverpool, L69 7ZD, U.K.

Received: June 14, 2004; In Final Form: October 18, 2004

Modern valence bond theory, in its spin coupled form, is used to elucidate the electronic rearrangements that take place during the course of the gas-phase hetero-Diels−Alder cycloaddition reaction of *s-cis*-acrolein (*cis*-1-oxabutadiene or *cis*-propeneal) and ethene. It is found that the most dramatic changes to the electronic structure occur in a relatively narrow interval of the reaction pathway soon after the transition state and that the system passes through a geometry at which it can be considered to be significantly aromatic. Although concerted, the reaction is markedly asynchronous, with the breaking of the carbon−oxygen π bond, and the formation of the new carbon−oxygen σ bond, "lagging behind" somewhat the other bond-making and bond-breaking processes.

Introduction

Heterodienes, such as α,β-unsaturated carbonyl compounds,[1] undergo synthetically useful 1,4-cycloadditions to dienophiles, such as alkenes, to produce six-membered rings containing heteroatoms. These thermally allowed [4+2] cycloadditions may be termed hetero-Diels−Alder reactions,[2] by analogy to the Diels−Alder reaction of *cis*-butadiene and ethene. In the present work, we use modern valence bond theory, in its spin-coupled (SC) form, to investigate the electronic mechanism of the gas-phase hetero-Diels−Alder cycloaddition reaction of *s-cis*-acrolein and ethene (see Scheme 1).

Computational Procedure

The geometry of the transition state (TS) for the gas-phase cycloaddition reaction between *s-cis*-acrolein (*cis*-1-oxabutadiene or *cis*-propeneal) and ethene was optimized using 6-31G(d) and 6-31G(d,p) basis sets with a variety of approaches, including the restricted Hartree−Fock (RHF), density functional theory (B3LYP), and second-order Møller−Plesset perturbation theory [MP2(fc)] levels of theory. Analogous calculations were also performed for *s-cis*-acrolein. Following an examination of the various results, the MP2/6-31G(d) approach was selected for mapping out the intrinsic reaction coordinate (IRC), starting from the TS and moving in steps of about 0.1 amu$^{1/2}$ bohr until local minima were reached in the directions of the reactants and of the product. All of these geometry optimizations were carried out using standard procedures in GAUSSIAN98,[3,4] with tight convergence criteria for the optimizations and default criteria for the IRC calculations. The authenticity of the various minima and saddle points was confirmed by examining the eigenvalues of the analytic Hessians.

We carried out spin-coupled (SC) calculations based on a single spatial configuration consisting of N fully optimized, nonorthogonal, one-electron "active" orbitals ψ_μ, together with a set of n fully optimized, orthogonal, doubly occupied

SCHEME 1

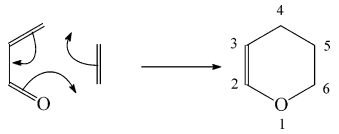

"inactive" orbitals ϕ_i. Such a wave function may be written in the general form[5]

$$\Psi = \hat{A}[(\sum_{i=1}^{n} \phi_i\alpha\phi_i\beta)(\sum_{\mu=1}^{N} \psi_\mu)\Theta_{SM}^{N}] \quad (1)$$

in which Θ_{SM}^{N} is the active-space spin function (for N electrons with total spin S and projection M) which is expanded in the full spin space, according to

$$\Theta_{SM}^{N} = \sum_{k=1}^{f_S^N} C_{Sk}\,\Theta_{SM;k}^{N} \quad (2)$$

The cycloaddition reaction formally involves a total of six active electrons, namely four π electrons from *s-cis*-acrolein and two from ethene, and so it was natural to choose these numbers for the values of N in the various SC calculations.

In classical VB approaches, each orbital is expanded only in terms of basis functions located on a particular atomic center. No such restrictions are imposed here on any of the active or inactive orbitals, which are entirely free to deform toward and to delocalize onto other centers. It is usual to label such a calculation "modern" valence bond. There are also no restrictions on the spin-coupling coefficients (C_{Sk}) in eq 2. All of the variational parameters, namely the C_{Sk} and the expansion coefficients of all the ψ_μ and ϕ_i orbitals in the underlying 6-31G(d) basis set, are optimized simultaneously. In general, the very compact SC wave functions with N active electrons are only slightly inferior to the corresponding 'N electrons in N orbitals' CASSCF descriptions, but they are of course a great deal simpler to interpret directly.

The spin-coupled calculations reported in the present work were performed using a version of our code[6] which works in

* To whom correspondence should be addressed. E-mail: dlc@liverpool.ac.uk (D.L.C.); pbk1@york.ac.uk (P.B.K.).
† University of York.
‡ University of Liverpool.

10.1021/jp047431e CCC: $30.25
Published on Web 12/08/2004

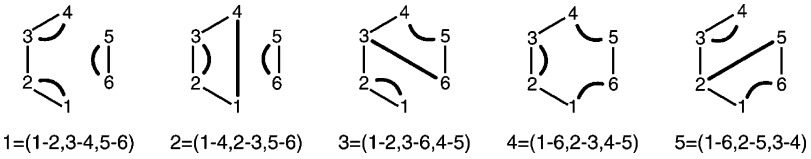

Figure 1. Rumer spin eigenfunctions included in the active-space spin-coupling pattern Θ^6_{00}.

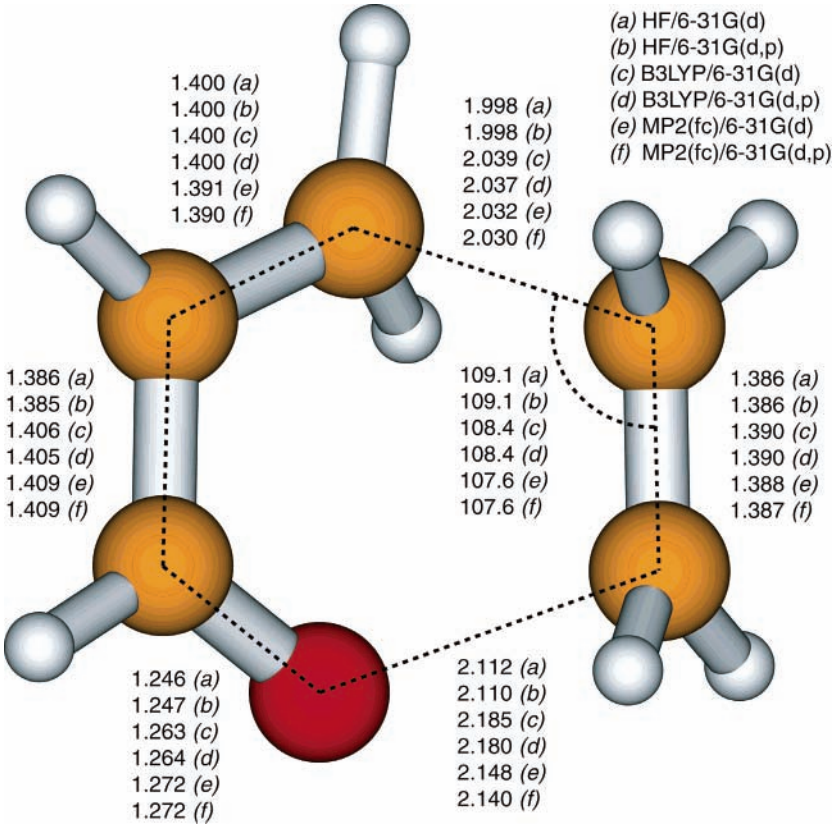

Figure 2. Key features of optimized geometries for the gas-phase transition state in the hetero-Diels−Alder reaction of *s-cis*-acrolein and ethene, with bond lengths in ångstroms and angles in degrees.

the Kotani spin basis,[7,8] but it proved more convenient for discussing the changes in the active-space spin-coupling patterns to transform instead to the more traditional Rumer basis[7,9] that has been widely used in classical VB calculations. The (exact) interconversion between different bases of spin eigenfunctions can be carried out through a specialized code for symbolic generation and manipulation of spin eigenfunctions, SPINS.[10] The relative importance of the different Rumer functions $\Theta^N_{SM;k}$ to the active-space spin function are conveniently quantified by means of their Chirgwin−Coulson weights,[11] P^{CC}_k, defined according to

$$P^{CC}_k = C_{Sk}\sum_{l=1}^{f^N_S} C_{Sl}\langle\Theta^N_{SM;k}|\Theta^N_{SM;l}\rangle \qquad (3)$$

For *s-cis*-acrolein, treated as a singlet species with four active π electrons, the active-space spin-coupling pattern is spanned by $f^4_0 = 2$ Rumer functions, which may be conveniently represented $\Theta^4_{00;1} \equiv$ (1-2,3-4) and $\Theta^4_{00;2} \equiv$ (1-4,2-3), in which $i-j$ denotes singlet coupling of the spins of electrons i and j. For the reacting system, with $N = 6$, $S = 0$ and $f^6_0 = 5$, Rumer functions $\Theta^6_{00;1} \equiv$ (1-2,3-4,5-6) and $\Theta^6_{00;4} \equiv$ (1-6,2-3,4-5) are reminiscent of the traditional Kekulé structures for benzene, as shown in Figure 1, and the three remaining Rumer functions, $\Theta^6_{00;2} \equiv$ (14,23,56), $\Theta^6_{00;3} \equiv$ (12,36,45) and $\Theta^6_{00;5} \equiv$ (16,25,34), are analogous to the corresponding Dewar-like structures.

Additional information may be obtained from the total (spinless) one-particle density matrix, **D**. In particular, we examine here the variation along the reaction pathway of the so-called generalized Wiberg or Wiberg−Mayer indices,[12−14] defined according to

$$W_{AB} = \sum_{p\in a}\sum_{q\in b}(\mathbf{DS})_{pq}(\mathbf{DS})_{qp} \qquad (4)$$

where **S** is the overlap matrix, and the notation $p\in a$ signifies all basis functions centered on atom A, with the atoms numbered as shown in Scheme 1. Such indices have proved most useful at the restricted Hartree−Fock level, where they have been employed as bond orders or bond indices to characterize the multiplicity of chemical bonds. Unfortunately, the absolute values of W_{AB} calculated from correlated wave functions are not so informative, but we may still usefully compare the relative magnitudes for different pairs of atoms. The main utility of the W_{AB} profiles is that they are expected to show inflection points in the region of the IRC where the bonding pattern is changing most rapidly.[14]

Results and Discussion

Key features of RHF, B3LYP and MP2(fc) transition state geometries for the gas-phase hetero-Diels−Alder cycloaddition reaction of *s-cis*-acrolein to ethene are summarized in Figure

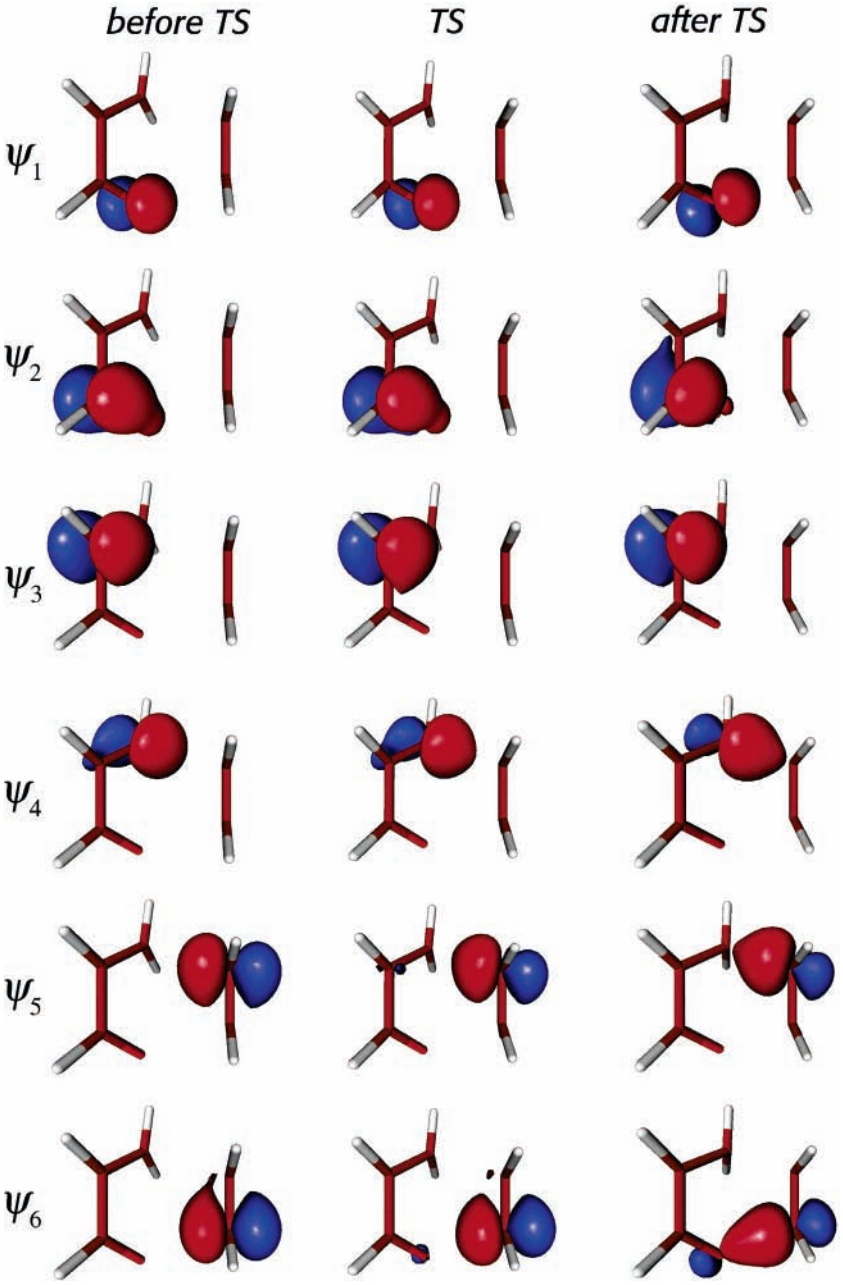

Figure 3. Active orbitals from SC/6-31G(d) calculations along the MP2/6-31G(d) IRC for the gas-phase cycloaddition reaction of *s-cis*-acrolein and ethene: early "before" −TS geometry at $R_{IRC} = -1.19482$ amu$^{1/2}$ bohr (left-hand column); TS geometry at $R_{IRC} = 0$ amu$^{1/2}$ bohr (central column); late "after" −TS geometry at $R_{IRC} = +1.19671$ amu$^{1/2}$ bohr (right-hand column). Three-dimensional isovalue surfaces corresponding to $\psi_\mu = \pm 0.1$ were drawn from the virtual reality modeling language (VRML) files produced by MOLDEN.[17]

2. Further results, obtained using quadratic configuration interaction (QCISD), coupled-cluster (CCD) and fourth-order Møller−Plesset (MP4(fc)) calculations, are also available.[15] At all of these levels of theory, the heavy-atom system is nonplanar, with the length of the forming carbon−oxygen σ bond ca. 0.1 Å greater than that of the forming carbon−carbon σ bond. Where appropriate, we checked that our results with the 6-31G(d) basis are consistent with those reported by Lee and co-workers.[2] On the whole, the changes to the geometry on expanding the basis to 6-31G(d,p) are fairly small, at all the levels of theory we considered. After careful examination of all these geometric data for the TS, we selected the MP2(fc)/6-31G(d) approach for the subsequent IRC calculations.

The key changes to the SC description of the electronic structure along the MP2/6-31G(d) reaction path may be deduced by monitoring the evolution of the shapes of the active SC orbitals, the overlaps between them, the weights of the different Rumer spin eigenfunctions, and the relative values of the generalized Wiberg indices. The SC active orbitals are depicted in Figure 3 for three geometries which are sufficiently well separated so as to highlight the key changes to the shapes of the orbitals. The left-hand column corresponds to an early "before" -TS geometry ($R_{IRC} \approx -1.2$ amu$^{1/2}$ bohr), the central column to the TS (at $R_{IRC} \approx 0$ amu$^{1/2}$ bohr) and the right-hand column to a late "after" -TS geometry ($R_{IRC} \approx 1.2$ amu$^{1/2}$ bohr). Although no such constraints were imposed in the calculations, we find for each geometry that the SC active orbitals are each associated with one heavy-atom center, and so it proves convenient to number them accordingly (see also Scheme 1).

As one would expect, the SC description of the separated reactants[15] is characterized by essentially three pairs of active orbitals, with predominantly singlet coupling of the correspond-

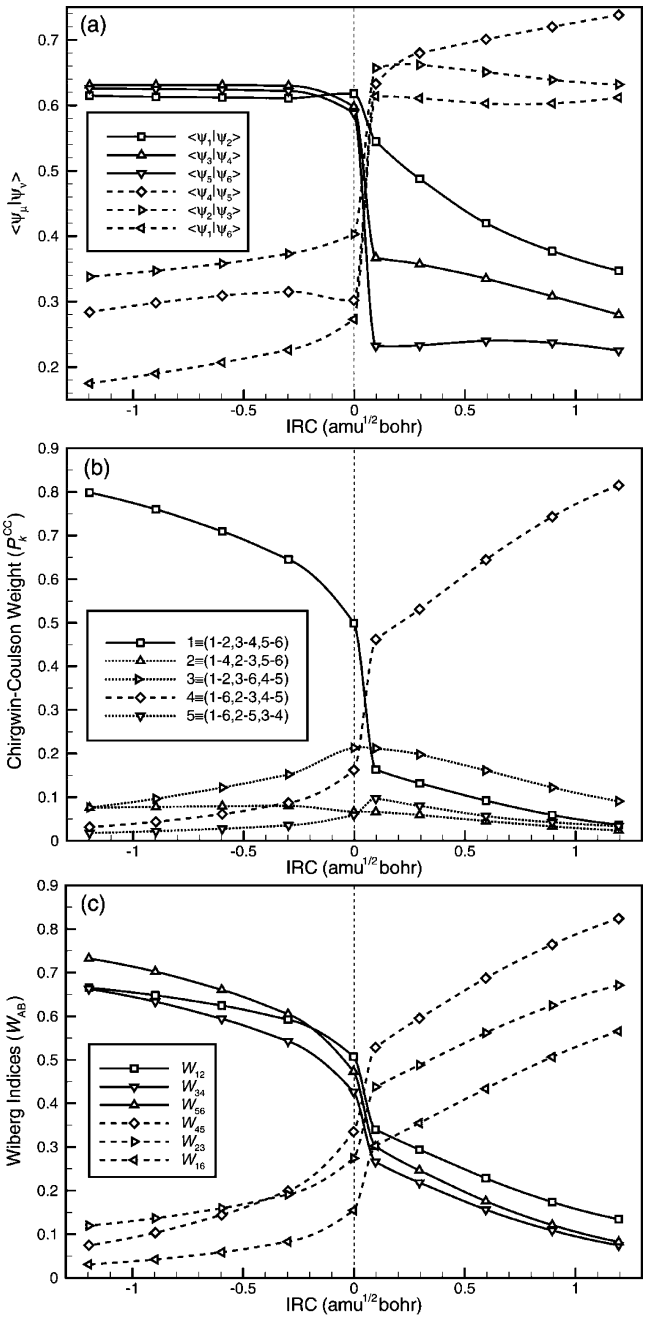

Figure 4. Evolution of key quantities along the MP2/6-31G(d) IRC for the gas-phase cycloaddition reaction of *s-cis*-acrolein and ethene: (a) overlap integrals $\langle\psi_\mu|\psi_\nu\rangle$ between nearest-neighbor active SC orbitals; (b) Chirgwin−Coulson weights (P_k^{CC}) of the Rumer spin functions included in the active-space spin-coupling pattern; (c) generalized Wiberg indices (W_{AB}) for nearest-neighbor atoms, numbered as in Scheme 1. The numbering and phases of the orbitals are shown in Figure 3, and the Rumer functions $\Theta^6_{00;k}$ are depicted in Figure 1. Numerical values are listed in the Supporting Information.

ing spins: (ψ_1,ψ_2) is associated with the acrolein carbon−oxygen π bond, (ψ_3,ψ_4) with the acrolein carbon−carbon π bond, and (ψ_5,ψ_6) with the ethene carbon−carbon π bond. This basic pattern is mostly preserved at the "before" -TS geometry for which orbitals are shown in the leftmost column of Figure 3. The overlaps within each pair are all above 0.6, and the reactant-like Kekulé Rumer function dominates the active-space spin-coupling pattern, with $P_1^{CC} = 0.80$. Even at this relatively early stage of the reaction, there are some signs of interactions between the orbitals of the two moieties. For example, the overlaps $\langle\psi_4|\psi_5\rangle$ and $\langle\psi_1|\psi_6\rangle$, which will correspond in due course to the newly formed carbon−carbon and carbon−oxygen σ bonds in the product, are already 0.28 and 0.18, respectively.

The central column in Figure 3 shows the active SC orbitals at the TS for the gas-phase hetero-Diels−Alder addition of *s-cis*-acrolein to ethene. Orbitals ψ_5 and ψ_6, which were initially responsible for the ethene carbon−carbon π bond, are now starting to become engaged in the new ring-closing σ bonds. Orbitals ψ_2 and ψ_3, which will form the carbon−carbon π bond in the product, show enhanced interaction with one another, with the relevant overlap integral increasing from 0.31 in the reactants, to 0.34 at the "before" -TS geometry, to 0.40 at the TS. It is clear, though, from Figure 4a that the most dramatic changes to the various overlap integrals do not occur until a little after the TS. Similarly, although the weight of the reactant-like Kekulé spin eigenfunction drops to $P_1^{CC} = 0.50$ at the TS, the most rapid changes to the active-space spin-coupling pattern (see Figure 4b) occur over a relatively short IRC interval at slightly later geometries, where the orbital overlaps are also changing most rapidly. The product-like Kekulé Rumer function still has a relatively small weight at the TS, $P_4^{CC} = 0.16$. Indeed, this value is slightly smaller than the contribution of $P_3^{CC} = 0.21$ from the Dewar-like Rumer spin eigenfunction that preserves the singlet coupling of the spins associated with the two electrons in the acrolein carbon−oxygen π bond. All of the numerical data used to construct Figure 4 are listed in the Supporting Information.

The forms of the SC active orbitals at the late "after" -TS geometry, shown in the right-hand column of Figure 3, correspond to essentially three pairs: (ψ_4,ψ_5) is associated with the ring-closing carbon−carbon σ bond, (ψ_1,ψ_6) with the ring-closing carbon−oxygen σ bond, and (ψ_2,ψ_3) with the new carbon−carbon π bond in the product. The overlap integrals within these three pairs are now 0.74, 0.61 and 0.63, respectively, and the nearest-neighbor overlaps between orbitals that were responsible for bonds in the reactants have all decreased significantly relative to the values at the TS. It is of course now the product-like Kekulé Rumer function that dominates the active-space spin-coupling pattern, with $P_4^{CC} = 0.81$. The second largest contributor is the Dewar-like spin eigenfunction $\Theta^6_{00;3} \equiv$ (1-2,3-6,4-5) albeit with a Chirgwin−Coulson weight of just 0.09, but we note that the overlap $\langle\psi_1|\psi_2\rangle$ is still almost 0.35 at this late geometry. The breaking of the carbon−oxygen π bond, and the formation of the new carbon−oxygen σ bond, clearly "lag behind" somewhat the other bond-making and bond-breaking processes. Although concerted, the reaction is certainly very asynchronous.

The rapid changes to the overlaps between the active SC orbitals, over a relatively short IRC interval soon after the TS (see Figure 4a), are accompanied by corresponding changes to the weights P_1^{CC} and P_4^{CC} (see Figure 4b) of the two Kekulé Rumer functions in the active-space spin-coupling pattern. As anticipated,[14] the generalized Wiberg index W_{AB} profiles (see Figure 4c) also show rapid changes in this region, with inflection points located at much the same value of R_{IRC} as are those for the orbital overlaps and spin function weights. Many of the overlaps attain fairly similar values in the vicinity of $R_{IRC} = -0.05$ amu$^{1/2}$ bohr, as also do many of the W_{AB} values, and the weights of the two Kekulé spin eigenfunctions also become equal. These various observations are of course strongly suggestive of "aromatic" character.

Summary and Conclusions

A series of SC/6-31G(d) calculations along the MP2(fc)/6-31G(d) IRC has been used to elucidate the electronic rearrange-

ments that take place during the course of the gas-phase hetero-Diels−Alder cycloaddition reaction of *s-cis*-acrolein. We examined the variation along the reaction pathway of the shapes of the SC active orbitals, and the overlaps between them, the weights of the different components in the active-space spin-coupling pattern, and the values of the generalized Wiberg indices. The different rates of the various changes show that this concerted reaction is markedly asynchronous, with the breaking of the carbon−oxygen π bond, and the formation of the new carbon−oxygen σ bond, "lagging behind" somewhat the other bond-making and bond-breaking processes.

As in the case of the Diels−Alder reaction of butadiene and ethene,[16] we find that this gas-phase process is homolytic, in the sense that each SC orbital remains distinctly associated with a single atomic center throughout the course of the reaction. It is thus tempting to represent the bond-breaking and bond-making by half arrows:

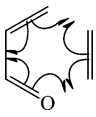

Our calculations show that the most dramatic changes to the electronic structure occur in a relatively narrow R_{IRC} interval soon after the TS, where the system passes through a geometry at which it can be considered to be significantly aromatic.

Supporting Information Available: Tables of numerical data used to construct Figure 4. This material is available free of charge via the Internet at http://pubs.acs.org.

References and Notes

(1) Desimoni, G.; Tacconi, G. *Chem. Rev.* **1975**, *75*, 651.
(2) Park, Y. S.; Lee, B.-S.; Lee, I. *New J. Chem.* **1999**, *23*, 707.
(3) Frisch, M. J.; Trucks, G. W.; Schlegel, H. B.; Scuseria, G. E.; Robb, M. A.; Cheeseman, J. R.; Zakrzewski, V. G.; Montgomery, J. A.; Stratmann, R. E.; Burant, J. C.; Dapprich, S.; Millam, J. M.; Daniels, A. D.; Kudin, K. N.; Strain, M. C.; Farkas, O.; Tomasi, J.; Barone, V.; Cossi, M.; Cammi, R.; Mennucci, B.; Pomelli, C.; Adamo, C.; Clifford, S.; Ochterski, J.; Petersson, G. A.; Ayala, P. Y.; Cui, Q.; Morokuma, K.; Malick, D. K.; Rabuck, A. D.; Raghavachari, K.; Foresman, J. B.; Cioslowski, J.; Ortiz, J. V.; Baboul, A. G.; Stefanov, B. B.; Liu, G.; Liashenko, A.; Piskorz, P.; Komaromi, I.; Gomperts, R.; Martin, R. L.; Fox, D. J.; Keith, T.; Al-Laham, M. A.; Peng, C. Y.; Nanayakkara, A.; Gonzalez, C.; Challacombe, M.; Gill, P. M. W.; Johnson, B.; Chen, W.; Wong, M. W.; Andres, J. L.; Head-Gordon, M.; Replogle, E. S.; Pople, J. A. Gaussian 98 (Revision A.7); Gaussian: Pittsburgh, PA, 1998.
(4) (a) Gonzalez, C.; Schlegel, H. B. *J. Chem. Phys.* **1989**, *90*, 2154. (b) Gonzalez, C.; Schlegel, H. B. *J. Phys. Chem.* **1990**, *94*, 5523.
(5) (a) Cooper, D. L.; Gerratt, J.; Raimondi, M. *Chem. Rev.* **1991**, *91*, 929. (b) Gerratt, J.; Cooper, D. L.; Karadakov, P. B.; Raimondi, M. In *Handbook of Molecular Physics and Quantum Chemistry*; Wilson, S., Ed.; Wiley: Chichester, U.K., 2003; Vol. 2, Part 2, Chapter 12, pp 148−68.
(6) Karadakov, P. B.; Gerratt, J.; Cooper, D. L.; Raimondi, M. *J. Chem. Phys.* **1992**, *97*, 7637.
(7) Pauncz, R. *Spin Eigenfunctions*; Plenum Press: New York, 1979.
(8) Kotani, M.; Amemyia, A.; Ishiguro, E.; Kimura, T. *Tables of Molecular Integrals*; Maruzen: Tokyo, 1963.
(9) Rumer, G. *Göttinger Nachr.* **1932**, *3*, 337.
(10) Karadakov, P. B.; Gerratt, J.; Cooper, D. L.; Raimondi, M. *Theor. Chim. Acta* **1995**, *90*, 51.
(11) Chirgwin, B. H.; Coulson, C. A. *Proc. R. Soc. London, Ser. A* **1950**, *201*, 196.
(12) Wiberg, K. N. *Tetrahedron* **1968**, *24*, 1083.
(13) Mayer, I. *Chem. Phys. Lett.* **1983**, *97*, 270.
(14) Ponec, R.; Yuzhakov, G.; Cooper, D. L. *J. Phys. Chem. A* **2003**, *107*, 2100 and references therein.
(15) Blavins, J. J. A Study into Pericyclic Reactions and beyond through the Lens of Modern Valence Bond Theory. Ph.D. Thesis, University of York, York, U.K., 2003. Geometry optimizations and SC results are also presented for *s-cis*-acrolein.
(16) Karadakov, P. B.; Cooper, D. L.; Gerratt, J. *J. Am. Chem. Soc.* **1998**, *120*, 3975.
(17) Schaftenaar, G. *MOLDEN (A Pre- and Postprocessing Program of Molecular and Electronic Structure)*; CAOS/CAMM Center: The Netherlands.